PHYSICAL REVIEW A **77**, 031401(R) (2008)

Ab initio theoretical investigation of the frequency comb structure and coherence in the vuv-xuv regimes via high-order harmonic generation

Juan J. Carrera,[1,2] Sang-Kil Son,[1] and Shih-I Chu[1,2,*]
[1]*Department of Chemistry, University of Kansas, Lawrence, Kansas 66045, USA*
[2]*Center for Theoretical Sciences, Department of Physics, National Taiwan University, Taipei, Taiwan*
(Received 10 April 2007; published 3 March 2008)

We present a fully *ab initio* quantum investigation of the frequency comb structure and coherence within each order of the high-order harmonic generation (HHG) spectrum in the high-frequency vuv-xuv regime. The HHG spectrum driven by a train of equal-spacing short laser pulses is calculated by propagating the time-dependent Schrödinger equation accurately and efficiently by means of the time-dependent generalized pseudospectral method. We explore the comb structure and coherence by varying the laser pulse separation τ, the number of pulses N, and the laser intensity. We find that a nested comb structure appears within each of the harmonics, ranging from the first harmonic all the way to the cutoff harmonic, and this global pattern persists regardless of the values of τ and N used. The comb structure of the harmonics originates from quantum interferences among induced dipole pulses. Finally, the frequency comb structure prevails even in the presence of appreciable ionization.

DOI: 10.1103/PhysRevA.77.031401 PACS number(s): 42.65.Ky, 31.15.A−, 32.80.Rm, 42.62.Eh

In the last several years, femtosecond laser-based optical frequency combs have led to remarkable advancements in ultrafast science [1,2] and high-precision optical frequency measurement and synthesis [3,4], and enabled optical atomic clocks [5,6]. As a universal optical frequency comb synthesizer, this method provides a direct link between optical and microwave frequencies [7–9]. Small-scale spectroscopy laboratories can now measure or synthesize any optical frequency with extreme precision. The femtosecond frequency comb techniques are also stimulating new frontiers in ultrafast science. Control of the wave form and phase evolution of few-cycle laser pulses [9,10] provides a powerful new tool for the study of highly nonlinear phenomena that depend on the carrier-envelope phase and the generation of soft-x-ray attosecond pulses by high-order harmonic generation (HHG) [2], etc. More recently, coherent extreme ultraviolet (xuv) [11] and vacuum ultraviolet (vuv) [12] radiation at a repetition frequency of more than 100 MHz, a 1000-fold improvement over previous experiments [13], has been generated via HHG. At such a repetition rate, the mode spacing of the frequency comb, which is expected to survive the HHG process, is large enough for high-resolution spectroscopy. If this is the case, there will be a number of other applications of such a quasicontinuous compact and coherent vuv-xuv source, including vuv-xuv holography, nanolithography, and x-ray atomic clocks, etc.

In this work we present the first *ab initio* theoretical exploration of the frequency comb structure and coherence in the vuv-xuv regimes via HHG. Although such a comb structure has been anticipated [11,12], there are currently experimental difficulties in the observation of the frequency comb structure within each harmonic, with the exception of the third-order harmonic case [12]. Experimentally, each atom gas injected into the focus of the resonator interacts with a sequence of equally time-spaced (τ) laser pulses before leaving the interaction region, resulting in intricate coherent effects to be studied. Thus the study of the frequency comb structure and the feasibility of observing such a structure within each high-order harmonic is of much current interest and significance, and can facilitate further experimental development of phase-coherent frequency combs in the vuv-xuv regimes.

To understand the mode structure of a frequency comb emitted by a mode-locked laser, consider the pulse circulating in a laser cavity [14]. Since the group and phase velocities inside the cavity are not equal, there is a phase shift $\Delta\phi$ from pulse to pulse. The angular frequency spectrum emanating from such a pulse train give rises to comb lines, spaced by the repetition frequency $\omega_r = 2\pi/\tau$ and the offset frequency $\omega_\delta = \Delta\phi/\tau$. The comb frequencies ω_m are given by

$$\omega_m = m\omega_r + \omega_\delta, \tag{1}$$

where m is an integer index and typically on the order of 10^5–10^6 [11].

To pursue the exploration of the detailed comb structure of each high-order harmonic, we perform accurate calculations of the time-dependent wave functions, induced dipole moments, and HHG spectra. Consider now the excitation of atomic hydrogen driven by a train of N pulses. The time-dependent Schrödinger equation (TDSE), in atomic units, is given by

$$i\frac{\partial}{\partial t}\psi(\mathbf{r},t) = \hat{H}(\mathbf{r},t)\psi(\mathbf{r},t) = [\hat{H}_0(\mathbf{r}) + \hat{V}(\mathbf{r},t)]\psi(\mathbf{r},t). \tag{2}$$

Here, $\hat{H}_0(\mathbf{r})$ is the field-free Hamiltonian, and $\hat{V}(\mathbf{r},t)$ is the time-dependent atom-field interaction. For a linearly polarized laser field of a pulse train ($\mathbf{F} \| \hat{z}$), $\hat{V}(\mathbf{r},t)$ can be expressed as

$$\hat{V}(\mathbf{r},t) = -\mathbf{F}\cdot\mathbf{r}E(t) = -FzE(t), \tag{3}$$

where

*sichu@ku.edu

$$E(t) = \sum_{n=1}^{N} \hat{E}(t - n\tau)\exp[i(\omega_c t - n\omega_c \tau + n\Delta\phi)]. \quad (4)$$

Here $\hat{E}(t)$ is the pulsed-train Gaussian envelope function, F is the laser electric field amplitude, ω_c is the carrier frequency, and N is the number of pulses. The pulse-to-pulse phase shift is given by $\Delta\phi$.

Equation (2) is solved accurately and efficiently by means of the time-dependent generalized pseudospectral (TDGPS) method [15]. The TDGPS technique has been successfully applied to the study of field-induced Rydberg-atom high-resolution spectroscopy [16], and strong-field HHG processes of atomic [15,17,18] and molecular [19] systems. The numerical scheme of the TDGPS method consists of two essential steps. (a) The spatial coordinates are optimally discretized in a *nonuniform* spatial grid by means of the generalized pseudospectral technique [20]. This discretization is characterized by denser grids near the nuclear origin and sparser grids for larger distances. (b) A second-order split-operator technique in the *energy* representation, which allows the explicit elimination of undesirable fast-oscillating high-energy components, is used for the efficient time propagation of the wave function [15],

$$\psi(\mathbf{r}, t + \Delta t) \simeq \exp[-i\hat{H}_0(\mathbf{r})\Delta t/2]\exp[-i\hat{V}(\mathbf{r}, t + \Delta t/2)\Delta t] \times \exp[-i\hat{H}_0(\mathbf{r})\Delta t/2]\psi(\mathbf{r}, t) + O(\Delta t^3). \quad (5)$$

The norm of the field-free wave function is preserved to at least ten digits of accuracy during the TDGPS time propagation of the wave function. For very long pulse separation, we can speed up the time propagation in the field-free time domain (between the pulses) as follows. Since $\hat{V}(\mathbf{r}, t) = 0$ in this time regime, Eq. (5) can be directly computed as $\psi(\mathbf{r}, t + \Delta t') \approx \exp[-i\hat{H}_0(\mathbf{r})\Delta t']\psi(\mathbf{r}, t)$, where $\Delta t' \gg \Delta t$. Having determined the time-dependent wave function $\psi(\mathbf{r}, t)$, we can then calculate the time-dependent induced dipole moment in the acceleration form [15],

$$d_A(t) = \left\langle \psi(\mathbf{r}, t) \left| -\frac{z}{r^3} + FE(t) \right| \psi(\mathbf{r}, t) \right\rangle, \quad (6)$$

from which the HHG intensity spectrum can be determined as follows:

$$S(\omega) = \frac{4\omega^4}{6\pi c^3}|\tilde{d}(\omega)|^2. \quad (7)$$

Here $\tilde{d}(\omega)$ is the Fourier transform of $d_A(t)$ divided by the number of pulses N to scale to the one-pulse case,

$$\tilde{d}(\omega) = \frac{1}{N\omega^2}\int_{-\infty}^{\infty} d_A(t)e^{-i\omega t}dt. \quad (8)$$

In the following we first compare the HHG spectrum for the one-pulse and five-sequential-pulse cases. The laser parameters used are 20 fs full width at half maximum (FWHM) Gaussian pulse(s), with wavelength $\lambda = 800$ nm, peak intensity $I = 10^{13}$ W/cm^2, and $\Delta\phi = \pi/4$. The time separation between the adjacent pulses is chosen to be $\tau = 0.5$ ps, corresponding to the repetition frequency ω_r of 3.04×10^{-4} a.u. or 2.00 THz. Such a pulse separation is chosen mainly to facilitate the calculation and will not affect the main comb structure and coherence patterns of the harmonics, as much longer pulse separations are subsequently considered. Figure 1(a) illustrates the laser pulse train of five Gaussian pulses separated by $\tau = 0.5$ ps. The corresponding ionization probability $[=1 - \langle\psi(\mathbf{r}, t)|\psi(\mathbf{r}, t)\rangle]$ is presented in Fig. 1(b). Partial ionization occurs during each period of the pulse excitation, and after each pulse is over, the ionization probability remains constant. We note that, at this relatively weak laser intensity, the ionization probability is very small and the survival probability is practically near unity. However, the effect of the pulse train on the HHG pattern is quite dramatic. Figure 1(c) shows the comparison of the HHG spectrum for the one- (dotted red curve) and five- (solid blue curve) pulse cases. For the one-pulse excitation, the HHG spectrum exhibits harmonics up to the 13th order. When the pulse train is used, a nested frequency comb structure is clearly discerned within each of the harmonic orders with the comb spectral spacing given by the repetition frequency ω_r. The frequency comb structure of the kth-order harmonic can be written as [11]

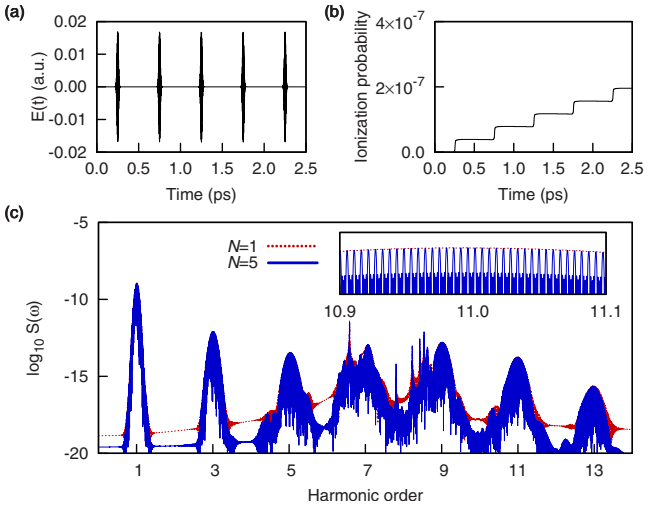

FIG. 1. (Color online) (a) Driving laser field of a train of five 20 fs FWHM Gaussian pulses interacting with H atoms. (b) Ionization probability of atomic H. (c) HHG spectrum generated by one pulse (dotted red line) and five pulses (solid blue line), and a detailed view (inset) of the nested comb structure in the vicinity of the 11th harmonic. Laser intensity used is 10^{13} W/cm^2, wavelength is 800 nm, and the time interval between the adjacent pulses is 0.5 ps.

$$\omega_l' = l\omega_r + k\omega_\delta, \quad (9)$$

where l is an integer index. We found that the pulse-to-pulse phase shift $\Delta\phi$ is preserved in all the harmonics, confirming the kth harmonic offset frequency $k\omega_\delta (= k\Delta\phi/\tau)$ in Eq. (9).

The inset of Fig. 1(c) displays the uniform comb frequency pattern around the 11th harmonic. Another notable feature is that the global envelope pattern of each of the harmonics is similar for the one- and five-pulse cases, and the harmonic intensity $S(\omega)$ of the five-pulse case at the comb's peak is very close to that of the one-pulse case. We

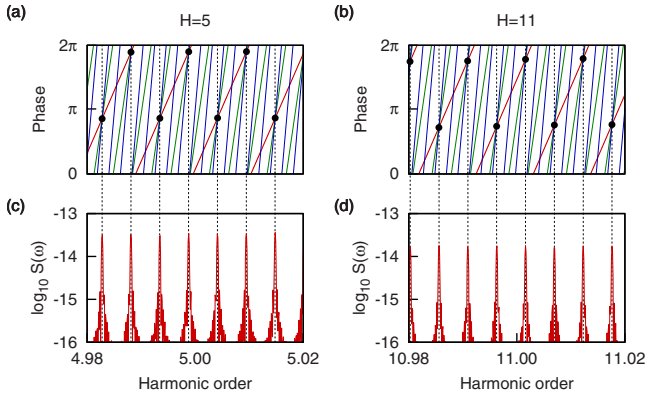

FIG. 2. (Color online) Spectral phases computed from the nth induced dipole pulse: (a) the fifth (H=5) and (b) the 11th (H=11) harmonics. The red line (the most slant) represents phases for the first dipole pulse ($n=1$), green line for $n=2$, and blue line (the least slant) for $n=3$. All lines intersect at the black dots indicating the comb positions. The corresponding frequency comb spectra for (c) H=5 and (d) H=11, computed with 20 pulses. Other laser parameters are the same as those in Fig. 1.

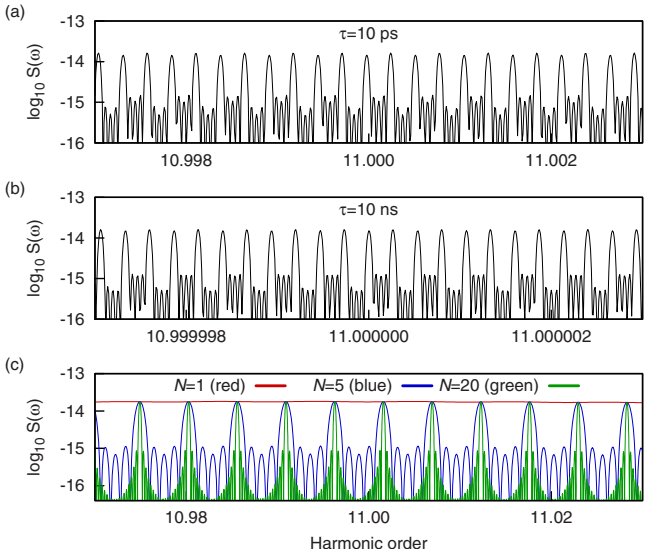

FIG. 3. (Color online) Frequency comb spectrum generated by a train of five ($N=5$) 20 fs FWHM Gaussian pulses near the 11th harmonic with varying time separation between pulses: τ=(a) 10 ps and (b) 10 ns. (c) The frequency comb structure for $N=1$, 5, and 20 pulse(s), respectively. Other laser parameters are the same as those in Fig. 1.

note that, as long as $N \geqslant 2$, the nested frequency comb structure will occur within each of the harmonics. To our knowledge, this is the first *ab initio* calculation exhibiting clearly the frequency comb structure within each of the high-order harmonics. This suggests that, with the improvement of the experimental resolution in the future, it is likely to be feasible to observe the frequency comb structure of high-order harmonics in the vuv-xuv regimes.

To understand the origin of harmonic comb generation, we perform an analysis of the spectral phases [14] of induced dipole moment pulses. The spectral dipole moment $\tilde{d}(\omega)$ in Eq. (8) can be decomposed into the components of each dipole pulse,

$$\tilde{d}(\omega) = \frac{1}{N}\sum_{n=1}^{N} \tilde{d}_n(\omega), \tag{10}$$

where $\tilde{d}_n(\omega)$ is computed from the nth dipole pulse,

$$\tilde{d}_n(\omega) = \frac{1}{\omega^2}\int_{(n-1)\tau}^{n\tau} d_A(t) e^{-i\omega t} dt. \tag{11}$$

The spectral phase $\theta_n(\omega)$ is defined as the phase of the complex spectral dipole $\tilde{d}_n(\omega)$: $\tilde{d}_n(\omega) = |\tilde{d}_n(\omega)| e^{i\theta_n(\omega)}$. $\theta_n(\omega)$ is plotted in Figs. 2(a) and 2(b) for the fifth and 11th harmonics, respectively. Constructive interference will occur only if the phases of individual dipole pulses are identical and intersect at the black dots where the comb positions are located in the corresponding frequency comb spectra shown in Figs. 2(c) and 2(d). These quantum interferences by the spectral phases generate the comb structure in all the harmonics.

We next investigate the effect of varying the time delay (pulse separation) τ on the coherent properties of the harmonics. Figures 3(a) and 3(b) show a comparison of the frequency comb spectrum (nearby the 11th harmonic) for the five-pulse case when the time delay is $\tau=10$ ps in Fig. 3(a), and 10 ns in Fig. 3(b). The 10 ns pulse separation corresponds to the typical experimental repetition frequency of 100 MHz. As the time delay is extended, we notice that the separation between comb modes decreases, since the repetition frequency ω_r is inversely proportional to τ [note the different scales of the x axes in Figs. 3(a) and 3(b)]. However, the harmonic intensity $S(\omega)$ at the comb's peak is nearly independent of τ. Phase coherence among excitation pulses essentially prevails as the time delay is prolonged.

We now study the effect on the frequency comb structure as the number of phase-locked pulses N is varied. Figure 3(c) shows the frequency comb structure for the cases of $N=1$, 5, and 20 pulses, respectively. The time delay is fixed at $\tau=0.5$ ps. The outline of the frequency comb spectrum (near the 11th harmonic) remains similar after the number of Gaussian pulses is varied: the number of comb frequency modes is exactly retained as N is varied. In addition, the harmonic intensity $S(\omega)$ is nearly independent of N in this relatively weak incident laser intensity case. However, the spectral width of each of the comb fringes γ_N $(=\tau/N)$ becomes narrower with increase of the number of pulses. Beyond this point, our results show that the coherence properties are essentially retained as the number of pulses is increased.

Consider now the coherence properties of the HHG comb structure in the presence of stronger laser intensity, $I=10^{14}$ W/cm^2, and $N=20$ pulses. Figure 4(a) shows the time-dependent ionization probability after the impact of 20 Gaussian pulses with $\tau=0.5$ ps. At this laser intensity, there is considerably more ionization occurring during each of the 20 pulses than in the weaker-intensity case. As the laser pulse train is completed, a staircaselike pattern best describes the overall form of the ionization probability. The corre-

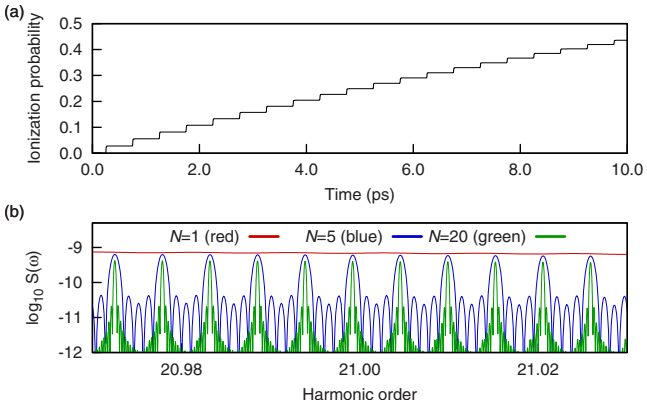

FIG. 4. (Color online) (a) Ionization probability after the impact of ($N=20$) 20 fs FWHM Gaussian pulse train. (b) Corresponding frequency comb spectrum around the 21st harmonic generated by the train of pulses for $N=1$, 5, and 20 pulse(s), respectively. Laser intensity is 10^{14} W/cm^2, and other laser parameters are the same as those in Fig. 1.

sponding frequency comb spectra for the train of $N=1$, 5, and 20 pulses in the vicinity of the 21st harmonic are shown in Fig. 4(b). We note that the harmonic intensity is slightly suppressed with increasing number of pulses. More importantly, the substantial ionization does not distort the coherence properties characterized by the smooth nested comb structure in any of the harmonics.

Last, we explore the sensitivity of the frequency comb structure as small perturbations are added to the driving laser field. We consider two decoherence cases: $\Delta\phi$ is perturbed, and τ is allowed to vary between pulses. The phase of the spectral dipole in Eq. (8) is governed by $(\omega\tau - k\Delta\phi)$, which can be verified from Eq. (9). The error of the phase when $\Delta\phi$ and τ are perturbed is proportional to $|\omega\tau|\delta(\tau)/\tau + |k\Delta\phi|\delta(\Delta\phi)/\Delta\phi$, where $\delta(\tau)/\tau$ and $\delta(\Delta\phi)/\Delta\phi$ are ratios (%) of small perturbations in τ and $\Delta\phi$, respectively. It shows that the phase will be more sensitive to τ than $\Delta\phi$, because $\omega\tau$ is typically large (for example, $\omega\tau = 2.3\times10^7$ at 800 nm and $\tau=10$ ns). Our calculations including small perturbations from pulse to pulse demonstrate that the uniform comb structure does not prevail if $\delta(\Delta\phi)/\Delta\phi > 0.1\%$ or $\delta(\tau)/\tau > 0.001\%$ when $\tau=1$ ps and the intensity of $I=10^{13}$ W/cm^2 used. This effect of decoherence is more dramatic as the intensity of the excitation fields becomes stronger. Furthermore, the coherence of the comb structure is more robust for the lower harmonics than for the cutoff harmonics.

In conclusion, we have presented a fully *ab initio* theoretical investigation of the frequency comb structure and coherence via HHG. The TDSE is accurately solved by means of the TDGPS method. We found that a nested comb structure appears within each of the harmonics, ranging from the first harmonic all the way to the cutoff harmonics. The comb structure arises from quantum interferences among induced dipole pulses. The frequency comb intensity $S(\omega)$ is nearly independent of the pulse separation τ and the number of pulses N used at weaker laser intensity. Also the comb structure prevails even when substantial ionization processes occur. This suggests that the experimental observation of the frequency comb structure in the vuv-xuv regimes will become possible when the spectral resolution is improved.

This work is partially supported by the Chemical Sciences, Geosciences and Biosciences Division of the Office of Basic Energy Sciences, Office of Sciences, U.S. Department of Energy, by the U.S. National Science Foundation, and by National Taiwan University. The authors would like to thank Dr. C. Gohle, Dr. R. J. Jones, Dr. J. Ye, and Dr. D. Telnov for valuable communications.

[1] M. Hentschel *et al.*, Nature (London) **414**, 509 (2001).
[2] M. Drescher *et al.*, Science **291**, 1923 (2001).
[3] M. Fischer *et al.*, Phys. Rev. Lett. **92**, 230802 (2004).
[4] H. S. Margolis *et al.*, Science **306**, 1355 (2004).
[5] M. Takamoto *et al.*, Nature (London) **435**, 321 (2005).
[6] S. A. Diddams *et al.*, Science **293**, 825 (2001).
[7] D. J. Jones *et al.*, Science **288**, 635 (2000).
[8] M. Niering *et al.*, Phys. Rev. Lett. **84**, 5496 (2000).
[9] R. Holzwarth *et al.*, Phys. Rev. Lett. **85**, 2264 (2000).
[10] A. Apolonski *et al.*, Phys. Rev. Lett. **85**, 740 (2000).
[11] C. Gohle *et al.*, Nature (London) **436**, 234 (2005).
[12] R. J. Jones, K. D. Moll, M. J. Thorpe, and J. Ye, Phys. Rev. Lett. **94**, 193201 (2005).
[13] F. Lindner *et al.*, Phys. Rev. A **68**, 013814 (2003).
[14] S. T. Cundiff and J. Ye, Rev. Mod. Phys. **75**, 325 (2003).
[15] X. M. Tong and S. I. Chu, Chem. Phys. **217**, 119 (1997).
[16] X. M. Tong and S. I. Chu, Phys. Rev. A **61**, 031401(R) (2000).
[17] X. M. Tong and S. I. Chu, Phys. Rev. A **61**, 021802(R) (2000); Phys. Rev. A **64**, 013417 (2001).
[18] J. J. Carrera, X. M. Tong, and S. I. Chu, Phys. Rev. A **74**, 023404 (2006).
[19] X. Chu and S. I. Chu, Phys. Rev. A **63**, 023411 (2001); **64**, 063404 (2001); **70**, 061402(R) (2004).
[20] G. Yao and S. I. Chu, Chem. Phys. Lett. **204**, 381 (1993).